

Communication

Iridium(triNHC)-Catalyzed Transfer Hydrogenation of Glycerol Carbonate without Exogenous Reductants

Yeon-Joo Cheong, Mi-hyun Lee, Heemin Byeon, Jiyong Park, Sungju Yu and Hye-Young Jang * 

Department of Energy Systems Research, Ajou University, Suwon 16499, Korea; mercedes02@ajou.ac.kr (Y.-J.C.); youncat486@ajou.ac.kr (M.-h.L.); bhm0602@ajou.ac.kr (H.B.); tqb8993@ajou.ac.kr (J.P.); sungjuyu@ajou.ac.kr (S.Y.)
* Correspondence: hyjang2@ajou.ac.kr; Tel.: +82-31-219-2555

Abstract: The iridium(Ir) (triNHC = tri-*N*-heterocyclic carbene)-catalyzed transfer hydrogenation of glycerol carbonate (GC) is described in the absence of additional hydride sources. The described reduction provides a sustainable route to produce industrially-valuable formate and lactate with high turnover numbers (TONs). The bimetallic Ir(I) involving triNHC carbene ligands exhibits high TONs, and the reaction mechanism, including the bimetallic Ir(triNHC) catalyst, is proposed based on mechanistic studies.

Keywords: CO₂; glycerol carbonate; formate; transfer hydrogenation; Ir(triNHC)



Citation: Cheong, Y.-J.; Lee, M.-h.; Byeon, H.; Park, J.; Yu, S.; Jang, H.-Y. Iridium(triNHC)-Catalyzed Transfer Hydrogenation of Glycerol Carbonate without Exogenous Reductants. *Catalysts* **2022**, *12*, 656. <https://doi.org/10.3390/catal12060656>

Academic Editor: Albert Poater

Received: 25 April 2022

Accepted: 13 June 2022

Published: 15 June 2022

Publisher's Note: MDPI stays neutral with regard to jurisdictional claims in published maps and institutional affiliations.



Copyright: © 2022 by the authors. Licensee MDPI, Basel, Switzerland. This article is an open access article distributed under the terms and conditions of the Creative Commons Attribution (CC BY) license (<https://creativecommons.org/licenses/by/4.0/>).

1. Introduction

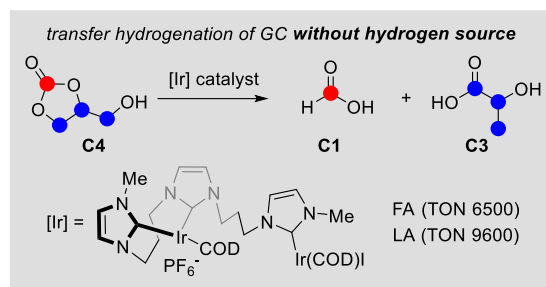
An indirect reduction in carbon dioxide (CO₂) via hydrogenation and transfer hydrogenation of organic carbonates is a practical and eco-friendly strategy that addresses global warming, plastic pollution, and energy problems by reducing the concentration of CO₂ in the air, recycling polycarbonate-based plastics, and producing valuable fuels and chemical feedstocks (formic acid, methanol, and diols) [1–5]. Thus, various transition metal-catalyzed reductions in organic carbonates have been studied, although organic carbonates are not highly susceptible to reduction. Ruthenium catalysts modified with tridentate ligands such as phosphorous-nitrogen-nitrogen (PNN) [6,7], phosphorous-nitrogen-phosphorous (PNP) [8,9], and carbon-nitrogen-carbon (CNC) [10], manganese catalysts involving PNN [11,12] and PNP [13] ligands, and cobalt catalysts containing nitrogen-oxygen coordinating ligands [14] are used to hydrogenate organic carbonates.

Although the transition metal-catalyzed hydrogenation of carbonates exhibits acceptable yields and catalytic activities, high pressure of H₂ (30–60 bar) should be applied, and the reactions must be run in the pressurized equipment. Thus, the isopropanol (IPA)-mediated reduction in organic carbonates, called transfer hydrogenation, is investigated. Ru(PNP) [15], Fe(PNP) [16], and Co(NO) [14] complexes have been used to reduce organic carbonates. In addition to transition metal-catalyzed hydrogenation and transfer hydrogenation, boron- and silane-mediated reduction in carbonates were reported in the presence of MgBu₂ [17], halide anions [18], and B(C₆F₅)₃ [19] catalysts.

For the transfer hydrogenation of organic carbonates, alcohols such as IPA and glycerol are required. IPA is a hydrogen source delivering hydrides to carbonates, generating reduced products (formic acid) and byproducts (acetone) formed from IPA [20]. Biomass-derived glycerol has been recently used for transfer hydrogenation with the environmental advantages of sustainable hydrogen sources. However, glycerol has not been employed to reduce organic carbonates [21,22]. Given that our research group has been studying glycerol-mediated transfer hydrogenation [23–25], the reaction of glycerol carbonate (GC) derived from CO₂ and glycerol has drawn our interest [26,27], where the additional reductants may not be required due to the glycerol moiety in GC.

As illustrated in Scheme 1, GC involves both C1 and C3 sources in the molecule. With a judicious choice of catalysts, GC plays C1 and C3 sources along with hydride

sources. The transfer hydrogenation of GC produces formate (C1 product) and lactate (C3 product), considered essential sustainable energy sources and bioplastic raw materials, respectively [28–31]. In this study, we report the first Ir(triNHC)-catalyzed transfer hydrogenation of GC in the absence of exogenous hydrides. The reaction mechanism is probed based on control experiments, and the origin of the high catalytic activity of bimetallic Ir(triNHC) was speculated based on the proposed reaction mechanism.



Scheme 1. Transfer hydrogenation of GC.

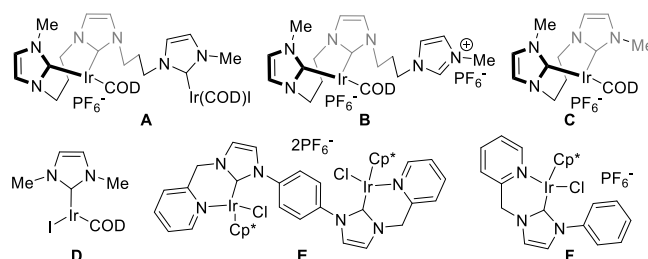
2. Results and Discussion

The reaction optimization results of transfer hydrogenation of GC are presented in Table 1. The reactions of GC, bases, and iridium catalysts were conducted in *N*-methyl-2-pyrrolidone (NMP) at 200 °C for 20 h. Catalysts **A–D** are reported [23,32–34], and catalysts **E** and **F** are newly synthesized. The optimization begins with different loadings of catalyst **A** and CsOH·H₂O (2 equiv.), showing turnover numbers (TONs) of 6500 (formate) and 9600 (lactate) with catalyst **A** (2.5×10^{-3} mol%) (entries 1–3). The TONs of formate and lactate were calculated by ¹H NMR spectroscopy in D₂O using isonicotinic acid as an internal standard (see Supplementary Materials Figure S5). Changing the solvent to H₂O diminished the catalytic activity (entry 4). Both NMP and water are commonly used solvents in the reactions of glycerol. Depending on the catalytic system, the optimized solvent was varied, and our catalytic system exhibited higher TONs in NMP. Although NMP can be converted to 4-*N*-methylaminobutanoate in the presence of bases, it has been known that 4-*N*-methylaminobutanoate does not affect the catalytic reaction of glycerol [35]. Different bases (KOH and NaOH) exhibit inferior results in terms of TONs of each product (entries 5 and 6). Increasing the amounts of CsOH·H₂O did not improve TONs (entry 7). In the absence of bases or catalysts, no product was observed (entries 8 and 9). The monometallic Ir catalysts **B–D** exhibit slightly lower TONs compared to bimetallic catalyst **A** (entry 10–13). The catalyst loadings of monometallic catalysts **B–D** were determined to maintain the same mole numbers of iridium ions of bimetallic catalyst **A**. Analogous to catalyst **A**, monometallic catalyst **B** showed increased TONs with lower catalyst loadings (entries 10 and 11). Ir(III) catalysts **E** and **F** involving the carbene, pyridine, and pentamethylcyclopentadiene (Cp*) show much lower TONs compared to Ir(I) catalysts **A–D** modified with carbene ligands (entries 14 and 15). The reactions of ethylene carbonate and propylene carbonate formed formate with TONs of 580 and 415, respectively, under the conditions of entry 2 (Table 1) (see Supplementary Materials Figures S6 and S7). Thus, the presence of a hydroxy group in GC is critical for high TONs. The stability of Ir(triNHC) (catalyst **A**) was evaluated by accumulation experiments, showing a slight decrease in TONs of each product in the second reaction (see Supplementary Materials Scheme S3).

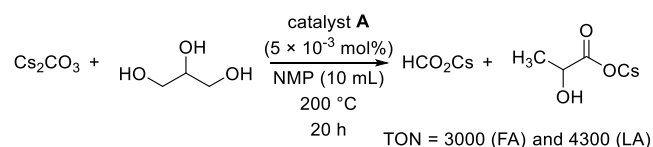
The mixture of catalysts, glycerol carbonate (10.6 mmol), and base in NMP (10 mL) was heated at 200 °C for 20 h. Catalysts **A** and **E** have two iridium ions in the molecule.

Table 1. Transfer hydrogenation of GC.

Entry	Catalyst (mol%)	Base (Equiv.)	Solvent	Formate (TON)	Lactate (TON)
1	A (2.5×10^{-3})	CsOH·H ₂ O (2)	NMP	6500	9600
2	A (5.0×10^{-3})	CsOH·H ₂ O (2)	NMP	3600	5300
3	A (1.0×10^{-2})	CsOH·H ₂ O (2)	NMP	980	1900
4	A (5.0×10^{-3})	CsOH·H ₂ O (2)	H ₂ O	21	89
5	A (5.0×10^{-3})	KOH (2)	NMP	12	65
6	A (5.0×10^{-3})	NaOH (2)	NMP	160	130
7	A (5.0×10^{-3})	CsOH·H ₂ O (3)	NMP	930	4800
8	A (5.0×10^{-3})	–	NMP	–	–
9	–	CsOH·H ₂ O (2)	NMP	–	–
10	B (1.0×10^{-2})	CsOH·H ₂ O (2)	NMP	2400	3600
11	B (5.0×10^{-3})	CsOH·H ₂ O (2)	NMP	5200	7400
12	C (1.0×10^{-2})	CsOH·H ₂ O (2)	NMP	2600	4200
13	D (1.0×10^{-2})	CsOH·H ₂ O (2)	NMP	2100	3400
14	E (5.0×10^{-3})	CsOH·H ₂ O (2)	NMP	580	2400
15	F (1.0×10^{-2})	CsOH·H ₂ O (2)	NMP	310	1700

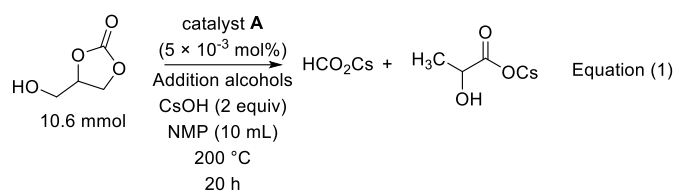


Control experiments were conducted to examine the transfer hydrogenation mechanism of GC (Schemes 2 and 3). Because GC might be dissociated to form glycerol and carbonates (CO_3^{2-}) in the presence of CsOH, the reactions of Cs_2CO_3 with glycerol were performed with catalyst A (Scheme 2). Compared to TONs of the GC reaction (FA = 3600, LA = 5300, entry 2 of Table 1), the reaction of Cs_2CO_3 with glycerol produces products with slightly lower TONs (FA = 3000 and LA = 4300). Thus, the reaction mechanism may involve the dissociation of GC into carbonate anions and glycerol.

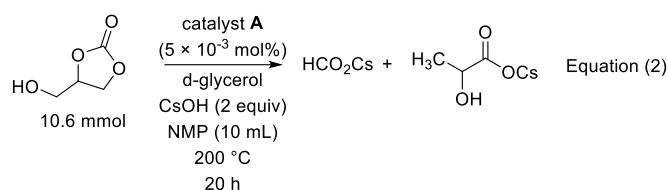
**Scheme 2.** Reaction of Cs_2CO_3 and glycerol.

The reactions of GC with additional alcohols (IPA and glycerol) were implemented with the assumption that an additional hydrogen source may increase the yields of formate and lactate. As depicted in Equation (1) of Scheme 3, the addition of IPA reduced the TONs of each product, and additional glycerol also slightly reduced the TONs of products. Because the additional alcohols reacted with catalysts and OH^- to induce dehydrogenation, glycerol carbonate reacted with reduced amounts of catalysts and bases, resulting in lower TONs of formate and lactate. An isotope labeling experiment using deuterated glycerol was conducted (Equation (2) of Scheme 3), forming small amounts of deuterated formate (approximately less than 10% by mass spectrometry analysis, see Supplementary Materials

Figure S8). Accordingly, most hydrogen atoms in the formate were derived from GC, and approximately 10% of external hydrogens were incorporated in the formate.



No additional alcohols: TONs = 3600 (FA), 5300 (LA)
 IPA (10.6 mmol): TONs = 2100 (FA), 3200 (LA)
 glycerol (10.6 mmol): TONs = 3100 (FA), 4900 (LA)



d-glycerol (10.6 mmol): TONs = 3300 (FA), 5300 (LA)

Scheme 3. Reaction of GC in the presence of additional alcohols.

The gas analysis of the reaction mixture was conducted to monitor the generation of CO_2 and H_2 from GC (Figure 1). Briefly, gaseous products were sampled from the headspace of the reactor at reaction times of 3 h and 20 h and then analyzed using gas chromatography. The number of moles of each product was determined from the area of the corresponding peak in the measured chromatogram. As depicted in Figure 1, H_2 gas (0.06 mmol) is generated at 3 h and 0.58 mmol at 20 h. The generated CO_2 was very low (as illustrated in the inset graph), where 0.53 and 0.31 μmol of CO_2 were observed at 3 and 20 h, respectively. During the reaction of GC, simple dehydrogenation forming H_2 gas is not a significant route based on the amount of generated H_2 (0.58 mmol) and used GC (10.6 mmol). The dissociation of CO_2 from GC rarely occurs based on the amount of liberated CO_2 . We exclude the hydrogenation of CO_2 as the main route of the mechanism because significant amounts of H_2 and CO_2 were not generated for the hydrogenation mechanism based on control experiments and gas analysis.

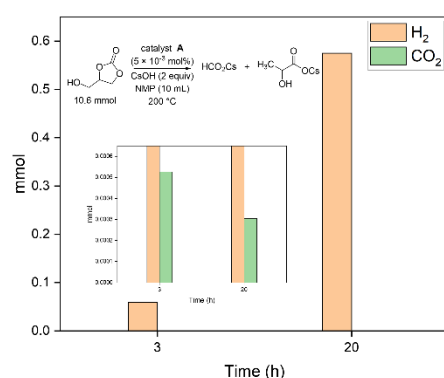
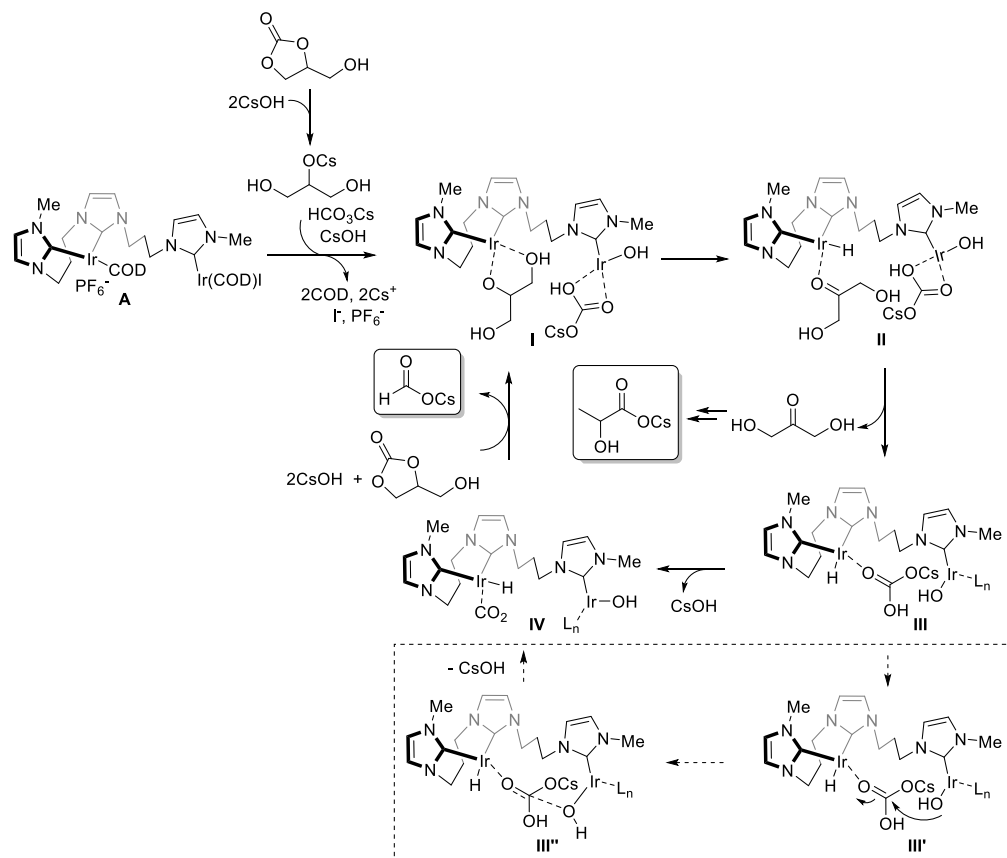


Figure 1. Gas analysis from the reaction mixture of glycerol carbonate, catalyst A, and CsOH.

We proposed a catalytic cycle of Ir(triNHC)-catalyzed transfer hydrogenation of GC (Scheme 4). Catalyst A releases cyclooctadiene (COD) and coordinates to the glycerol alkoxide and bicarbonate [23]. Glycerol alkoxides and bicarbonates are formed from GC and OH^- based on ^{13}C NMR of the mixture of GC and OH^- (see Supplementary Materials Figure S9). Intermediate I undergoes β -hydrogen elimination to produce intermediate II. Dihydroxyacetone (DHA) dissociated from intermediate II is converted to lactate via dehydration and Cannizzaro reaction [36]. The elimination of CsOH from intermediate III affords CO_2 -bound intermediate IV. The co-operative interaction of two iridium ions in

intermediate **III** promotes the elimination of CsOH via intermediates **III'** and **III''** [37,38]. The hydrometallation of CO₂ produces formic acid. GC and CsOH enter the catalytic cycle after releasing formates. The bimetallic catalysts showed higher TONs than monometallic catalysts; catalyst **A** vs. catalysts **B–D**. The efficient reaction of Ir-H with CO₂ might be promoted by the co-operative action of two iridium ions in the bimetallic catalyst's reaction sphere.



Scheme 4. Plausible reaction mechanism.

3. Conclusions

We report the first transfer hydrogenation of GC without additional hydrogen sources to the best of our knowledge. The control experiments and gas analysis confirm the reduction route induced by Ir(triNHC) catalysts. The reaction results of GC with deuterated glycerol imply that dissociated bicarbonates and glycerol alkoxides from GC are readily reacted before the participation of the external hydride sources in the reaction. The bimetallic catalysts are favored in coordinating both reactants (bicarbonates and glycerol alkoxides) inside the reaction sphere, as illustrated in the proposed reaction mechanism.

Supplementary Materials: The following supporting information can be downloaded at: <https://www.mdpi.com/article/10.3390/catal12060656/s1>, Scheme S1. The reaction of ethylene carbonate, Scheme S2. The reaction of propylene carbonate, Scheme S3. Accumulation experiments of GC and OH⁻, Table S1. Transfer hydrogenation of glycerol carbonate, Figure S1. ¹H NMR spectra of catalyst **E**, Figure S2. ¹³C NMR spectra of catalyst **E**, Figure S3. ¹H NMR spectra of catalyst **F**, Figure S4. ¹³C NMR spectra of catalyst **F**, Figure S5. ¹H NMR spectra of Entry 2 (Table 1) indicating the signature peak of each species, Figure S6. ¹H NMR spectra of the reaction mixture using ethylene glycol, Figure S7. ¹H NMR spectra of the reaction mixture using propylene glycol, Figure S8. Mass spectrum of the reaction mixture involving *d*-glycerol, Figure S9. ¹³C NMR spectra; glycerol (green), CsHCO₃ (red), the mixture of glycerol carbonate (GC) and CsOH (blue) and GC (black), Figure S10. ¹H NMR spectra in DMSO-*d*₆; (a) glycerol carbonate (green), (b) glycerol (blue), (c) catalyst **A** (red),

and (d) the mixture of glycerol carbonate (1 equiv), CsOH (2 equiv), catalyst A (0.5 equiv) (black). References [23,33,34] have been in the Supplementary Materials.

Author Contributions: Conceptualization, H.-Y.J.; Investigations, Y.-J.C., M.-h.L., H.B., J.P. and S.Y.; writing—original draft preparation, H.-Y.J.; writing—review and editing, H.-Y.J. All authors have read and agreed to the published version of the manuscript.

Funding: This research was funded by National Research Foundation of Korea, grant number 2020M3H7A1098283 and 2022R1A2C1004387.

Data Availability Statement: The data presented in this study are openly available in the Supplementary Materials.

Acknowledgments: This study was supported by the Carbon to X Program (No. 2020M3H7A1098283) and Basic Science Research Program (No. 2022R1A2C1004387) by the National Research Foundation of Korea, which is funded by the Ministry of Science and ICT).

Conflicts of Interest: The authors declare no conflict of interest.

References

1. Sordakis, K.; Tang, C.; Vogt, L.K.; Junge, H.; Dyson, P.J.; Beller, M.; Laurenczy, G. Homogeneous catalysis for sustainable hydrogen storage in formic acid and alcohols. *Chem. Rev.* **2018**, *118*, 372–433. [[CrossRef](#)] [[PubMed](#)]
2. Jessop, P.G.; Ikariya, T.; Noyori, R. Homogeneous hydrogenation of carbon-dioxide. *Chem. Rev.* **1995**, *95*, 259–272. [[CrossRef](#)]
3. Jessop, P.G.; Joó, F.; Tai, C.C. Recent advances in the homogeneous hydrogenation of carbon dioxide. *Coord. Chem. Rev.* **2004**, *248*, 2425–2442. [[CrossRef](#)]
4. Wang, W.-H.; Himeda, Y.; Muckerman, J.T.; Manbeck, G.F.; Fujita, E. CO₂ Hydrogenation to formate and methanol as an alternative to photo- and electrochemical CO₂ reduction. *Chem. Rev.* **2015**, *115*, 12936–12973. [[CrossRef](#)]
5. Dabral, S.; Schaub, T. The use of carbon dioxide (CO₂) as a building block in organic synthesis from an industrial perspective. *Adv. Synth. Catal.* **2019**, *361*, 223–246. [[CrossRef](#)]
6. Balaraman, E.; Gunanathan, C.; Zhang, J.; Shimon, L.J.W.; Milstein, D. Efficient hydrogenation of organic carbonates, carbamates and formates indicates alternative routes to methanol based on CO₂ and CO. *Nat. Chem.* **2011**, *3*, 609–614. [[CrossRef](#)]
7. Krall, E.M.; Klein, T.W.; Andersen, R.J.; Nett, A.J.; Glasgow, R.W.; Reader, D.S.; Dauphinais, B.C.; Mc Ilrath, S.P.; Fischer, A.A.; Carney, M.J.; et al. Controlled hydrogenative depolymerization of polyesters and polycarbonates catalyzed by ruthenium(II) PNN pincer complexes. *Chem. Commun.* **2014**, *50*, 4884–4887. [[CrossRef](#)]
8. Han, Z.; Rong, L.; Wu, J.; Zhang, L.; Wang, Z.; Ding, K. Catalytic hydrogenation of cyclic carbonates: A practical approach from CO₂ and epoxides to methanol and diols. *Angew. Chem. Int. Ed.* **2012**, *51*, 13041–13045. [[CrossRef](#)]
9. Li, Y.; Junge, K.; Beller, M. Improving the efficiency of the hydrogenation of carbonates and carbon dioxide to methanol. *ChemCatChem* **2013**, *5*, 1072–1074. [[CrossRef](#)]
10. Wu, X.; Ji, L.; Ji, Y.; Elageed, E.H.M.; Gao, G. Hydrogenation of ethylene carbonate catalyzed by lutidine-bridged N-heterocyclic carbene ligands and ruthenium precursors. *Catal. Commun.* **2016**, *85*, 57–60. [[CrossRef](#)]
11. Kumar, A.; Janes, T.; Espinosa-Jalapa, N.A.; Milstein, D. Manganese catalyzed hydrogenation of organic carbonates to methanol and alcohols. *Angew. Chem. Int. Ed.* **2018**, *57*, 12076–12080. [[CrossRef](#)] [[PubMed](#)]
12. Zubar, V.; Levedev, Y.; Azofra, L.M.; Cavallo, L.; El-Sepelgy, O.; Rueping, M. Hydrogenation of CO₂-derived carbonates and polycarbonates to methanol and diols by metal-ligand cooperative manganese catalysis. *Angew. Chem. Int. Ed.* **2018**, *57*, 13439–13443. [[CrossRef](#)] [[PubMed](#)]
13. Kaithal, A.; Hölscher, M.; Leitner, W. Catalytic hydrogenation of cyclic carbonates using manganese complexes. *Angew. Chem. Int. Ed.* **2018**, *57*, 13449–13453. [[CrossRef](#)] [[PubMed](#)]
14. Dahiya, P.; Gangwar, M.K.; Sundararaju, B. Well-defined Cp*Co(III)-catalyzed hydrogenation of carbonates and polycarbonates. *ChemCatChem* **2021**, *13*, 934–939. [[CrossRef](#)]
15. Kim, S.H.; Hong, S.H. Transfer hydrogenation of organic formates and cyclic carbonates: An alternative route to methanol from carbon dioxide. *ACS Catal.* **2014**, *4*, 3630–3636. [[CrossRef](#)]
16. Liu, X.; de Vries, J.G.; Werner, T. Transfer hydrogenation of cyclic carbonates and polycarbonate to methanol and diols by iron pincer catalysts. *Green Chem.* **2019**, *21*, 5248–5255. [[CrossRef](#)]
17. Szewczyk, M.; Magre, M.; Zubar, V.; Rueping, M. Reduction of cyclic and linear organic carbonates using a readily available magnesium catalyst. *ACS Catal.* **2019**, *9*, 11634–11639. [[CrossRef](#)]
18. Bobbink, F.D.; Menoud, F.; Dyson, P.J. Synthesis of methanol and diols from CO₂ via cyclic carbonates under metal-free, ambient pressure, and solvent-free conditions. *ACS Sustain. Chem. Eng.* **2018**, *6*, 12119–12123. [[CrossRef](#)]
19. Feghali, E.; Cantat, T. Room temperature organocatalyzed reductive depolymerization of waste polyethers, polyesters, and polycarbonates. *ChemSusChem* **2015**, *8*, 980–984. [[CrossRef](#)]
20. Zassinovich, G.; Mestroni, G.; Gladiali, S. Asymmetric hydrogen transfer reactions promoted by homogeneous transition metal catalysis. *Chem. Rev.* **1992**, *92*, 1051–1069. [[CrossRef](#)]

21. Díaz-Álvarez, A.E.; Cadierno, V. Glycerol: A promising green solvent and reducing agent for metal-catalyzed transfer hydrogenation reactions and nanoparticles formation. *Appl. Sci.* **2013**, *3*, 55–69. [[CrossRef](#)]
22. Crabtree, R.H. Transfer hydrogenation with glycerol as H-donor: Catalyst activation, deactivation and homogeneity. *ACS Sustain. Chem. Eng.* **2019**, *7*, 15845–15853. [[CrossRef](#)]
23. Cheong, Y.-J.; Sung, K.; Park, S.; Jung, J.; Jang, H.-Y. Valorization of chemical wastes: Ir(biscarbene)-catalyzed transfer hydrogenation of inorganic carbonates using glycerol. *ACS Sustain. Chem. Eng.* **2020**, *8*, 6972–6978. [[CrossRef](#)]
24. Sung, K.; Lee, M.-h.; Cheong, Y.-J.; Jang, H.-Y. Ir(triscarbene)-catalyzed sustainable transfer hydrogenation of levulinic acid to γ -valerolactone. *Appl. Organomet. Chem.* **2020**, *35*, e6105. [[CrossRef](#)]
25. Cheong, Y.-J.; Sung, K.; Kim, J.-A.; Kim, Y.K.; Yoon, W.; Yun, H.; Jang, H.-Y. Iridium(NHC)-catalyzed sustainable transfer hydrogenation of CO₂ and inorganic carbonates. *Catalysts* **2021**, *11*, 695. [[CrossRef](#)]
26. Christy, S.; Noschese, A.; Lomelí-Rodríguez, M.; Greeves, N.; Lopez-Sanchez, J.A. Recent progress in the synthesis and applications of glycerol carbonate. *Curr. Opin. Green Sustain. Chem.* **2018**, *14*, 99–107. [[CrossRef](#)]
27. Szöri, M.; Giri, B.R.; Wang, Z.; Dawood, A.E.; Viskolcz, B.; Farooq, A. Glycerol carbonate as a fuel additive for a sustainable future. *Sustain. Energy Fuels* **2018**, *2*, 2171–2178. [[CrossRef](#)]
28. Loges, B.; Boddien, A.; Gartner, F.; Junge, H.; Beller, M. Catalytic generation of hydrogen from formic acid and its derivatives: Useful hydrogen storage materials. *Top. Catal.* **2010**, *53*, 902–914. [[CrossRef](#)]
29. Grasmann, M.; Laurenczy, G. Formic acid as a hydrogen source-recent developments and future trends. *Energy Environ. Sci.* **2012**, *5*, 8171–8181. [[CrossRef](#)]
30. Mellmann, D.; Sponholz, P.; Junge, H.; Beller, M. Formic acid as a hydrogen storage material-development of homogeneous catalysts for selective hydrogen release. *Chem. Soc. Rev.* **2016**, *45*, 3954–3988. [[CrossRef](#)]
31. Bottari, G.; Barta, K. Lactic acid and hydrogen from glycerol via acceptorless dehydrogenation using homogeneous catalysts. *Recycl. Catal.* **2015**, *2*, 70–77. [[CrossRef](#)]
32. Frey, G.D.; Rentzsch, C.F.; von Preysing, D.; Scherg, T.; Mühlhofer, M.; Herdtweck, E.; Herrmann, W.A. Rhodium and iridium complexes of *N*-heterocyclic carbenes: Structural investigations and their catalytic properties in the borylation reaction. *J. Organomet. Chem.* **2006**, *691*, 5725–5738. [[CrossRef](#)]
33. Sharninghausen, L.S.; Campos, J.; Manas, M.G.; Crabtree, R.H. Efficient selective and atom economic catalytic conversion of glycerol to lactic acid. *Nat. Commun.* **2014**, *5*, 5084. [[CrossRef](#)] [[PubMed](#)]
34. Cheong, Y.-J.; Sung, K.; Kim, J.-A.; Kim, Y.K.; Jang, H.-Y. Highly efficient iridium-catalyzed production of hydrogen and lactate from glycerol: Rapid hydrogen evolution by bimetallic iridium catalysts. *Eur. J. Inorg. Chem.* **2020**, *2020*, 4064–4068. [[CrossRef](#)]
35. Sharninghausen, L.S.; Mercado, B.Q.; Crabtree, R.H.; Hazari, N. Selective conversion of glycerol to lactic acid with iron pincer precatalysts. *Chem. Commun.* **2015**, *51*, 16201–16204. [[CrossRef](#)]
36. Lu, Z.; Cherepakhin, V.; Demianets, I.; Lauridsen, P.J.; Williams, T.J. Iridium-based hydride transfer catalysts: From hydrogen storage to fine chemicals. *Chem. Commun.* **2018**, *54*, 7711–7724. [[CrossRef](#)]
37. Truscott, B.J.; Kruger, H.; Webb, P.B.; Bühl, M.; Nolan, S.P. The mechanism of CO₂ insertion into iridium(I) hydroxide and alkoxide bonds: A kinetics and computational study. *Chem. Eur. J.* **2015**, *21*, 6930–6935. [[CrossRef](#)]
38. Vummaleti, S.V.C.; Talarico, G.; Nolan, S.P.; Cavallo, L.; Poater, A. Mechanism of CO₂ fixation by Ir^I-X bonds (X = OH, OR, N, C). *Eur. J. Inorg. Chem.* **2015**, *2015*, 4653–4657. [[CrossRef](#)]